

This copy is for your personal, non-commercial use only.

If you wish to distribute this article to others, you can order high-quality copies for your colleagues, clients, or customers by [clicking here](#).

Permission to republish or repurpose articles or portions of articles can be obtained by following the guidelines [here](#).

The following resources related to this article are available online at www.sciencemag.org (this information is current as of September 22, 2011):

Updated information and services, including high-resolution figures, can be found in the online version of this article at:

<http://www.sciencemag.org/content/311/5759/371.full.html>

Supporting Online Material can be found at:

<http://www.sciencemag.org/content/suppl/2006/02/02/311.5759.371.DC1.html>

This article has been **cited by** 28 article(s) on the ISI Web of Science

This article has been **cited by** 6 articles hosted by HighWire Press; see:

<http://www.sciencemag.org/content/311/5759/371.full.html#related-urls>

This article appears in the following **subject collections**:

Microbiology

<http://www.sciencemag.org/cgi/collection/microbio>

polar deposits (24) and climate model simulations with orbital parameters different than today (25) suggest that the south polar region could also have played this role. On this basis, we performed a high-obliquity simulation assuming that ice was available in the south polar region (between 90°S and 80°S) rather than in the north. Under such conditions, ice accumulation still occurs in the southern part of Tharsis (Arsia-Pavonis Montes region and in Syria Planum), but the highest rates are then predicted to be in the eastern Hellas region (Fig. 4), almost exactly where the concentration of ice-related landforms is observed. Interestingly, the process leading to ice precipitation differs from the one occurring on the volcanoes. In eastern Hellas, almost all the ice is accumulated during a 90-day period around southern summer solstice (Fig. 2). At that time, the southern ice cap sublimates and releases large amounts of water vapor to the polar atmosphere. This water vapor is not easily transported toward the equator because the south polar region is isolated by a midlatitude westward summer vortex (26, 27), except near eastern Hellas. There, the deep Hellas Basin forces a stationary planetary wave that results in a strong northward flow that transports large amounts of water out of the polar region (fig. S2). The moist and warm polar air meets colder air coming from northern Hellas, and the subsequent cooling results in strong condensation and precipitation (Fig. 4 and fig. S3). This is a robust mechanism that should not be model-dependent (28).

For all the simulations presented here, some quantitative uncertainties remain, because our model is designed to simulate present-day Mars and does not include some processes that may be substantial at high obliquity, like the radiative feedback of water vapor and ice clouds or the scavenging of dust out of the atmosphere. The amount of dust lifted into the atmosphere may also have been different (28, 29). Additional simulations suggest that more atmospheric dust means less ice condensation because dust tends to warm the atmosphere.

The formation of glaciers on Mars appears to be the product of the same martian climate system as that of today, except that high obliquity increases the atmospheric water content and amplifies the circulation. In reality, the complex variations of orbital parameters probably led to several different types of regimes in the past, with water ice alternatively mobilized from the poles to tropical and midlatitude glaciers and then back to high latitudes to possibly form the meters-thick deposits whose remnants have been detected by the Mars Odyssey Gamma Ray Spectrometer (16). We do not predict glacier formation in the Deuteronilus-Protonilus Mensae area and other similar areas in the northern midlatitudes. These accumulations might have in-

involved climate changes due to other origins (impacts, volcanism, or catastrophic outflows). However, some combination of orbital parameters or a higher model resolution may be sufficient to simulate ice precipitation in this region without invoking other processes. The mobilization of ice to the low and midlatitudes in preferred locations such as Eastern Hellas also supports a simple, purely atmospheric scenario for the origin of many of the martian gullies (29).

References and Notes

- J. W. Head *et al.*, *Nature* **434**, 346 (2005).
- G. Neukum *et al.*, *Nature* **432**, 971 (2004).
- J. W. Head, D. R. Marchant, *Geology* **31**, 641 (2003).
- D. E. Shean, J. W. Head, D. R. Marchant, *J. Geophys. Res.* **110**, E05001 (2005).
- T. L. Pierce, D. A. Crown, *Icarus* **163**, 46 (2003).
- W. K. Hartmann, T. Thorsteinsson, F. Sigurdsson, *Icarus* **162**, 259 (2003).
- E. Hauber *et al.*, *Nature* **434**, 356 (2005).
- S. M. Milkovich, J. W. Head, D. R. Marchant, *Icarus*, in press.
- S. W. Squyres, *J. Geophys. Res.* **84**, 8087 (1979).
- B. K. Lucchitta, *Icarus* **45**, 264 (1981).
- P. R. Christensen, *Nature* **422**, 45 (2003).
- B. K. Lucchitta, *J. Geophys. Res.* **89** (suppl.), 409 (1984).
- N. Mangold, *J. Geophys. Res.* **108**, 10.1029/2002JE001885 (2003).
- B. M. Jakosky, M. H. Carr, *Nature* **315**, 559 (1985).
- M. A. Mischna, M. I. Richardson, R. J. Wilson, D. J. McCleese, *J. Geophys. Res.* **108**, 16-1 (2003).
- B. Levard, F. Forget, F. Montmessin, J. Laskar, *Nature* **431**, 1072 (2004).
- F. Forget *et al.*, *J. Geophys. Res.* **104**, 24155 (1999).
- F. Montmessin, F. Forget, P. Rannou, M. Cabane, R. M. Haberle, *J. Geophys. Res.* **109**, E10004 (2004).
- The visible dust optical depth is a measure of the amount of dust in the atmosphere. It is defined as the logarithm of the vertical extinction of radiation.
- J. Laskar *et al.*, *Icarus* **170**, 343 (2004).
- In practice, because such a model is too computationally expensive to be run for more than 2 years, we initialized the high-resolution simulation with the atmospheric water vapor predicted at the end of a 10-year identical run but performed the simulation with a lower resolution (3.75° by 5.625°). We then ran the model for 2 additional years at high resolution, at which point the atmosphere had come to an interannually repeatable state.
- M. I. Richardson, R. J. Wilson, *J. Geophys. Res.* **107**, 7-1 (2002).
- R. T. Clancy, M. J. Wolff, P. R. Christensen, *J. Geophys. Res.* **108**, 2-1 (2003).
- P. Thomas, S. Squyres, K. Herkenhoff, A. Howard, B. Murray, in *Mars*, H. H. Kieffer *et al.*, Eds. (Univ. of Arizona Press, Tucson, 1992), pp. 767-795.
- F. Montmessin, R. M. Haberle, F. Forget, *Proc. Lunar Planet. Sci. Conf.* **35**, 1312 (2004).
- R. M. Haberle, J. R. Murphy, J. Schaeffer, *Icarus* **161**, 66 (2003).
- C. E. Newman, S. R. Lewis, P. L. Read, *Icarus* **174**, 135 (2005).
- Additional simulations performed with more atmospheric water provided to the system by assuming a south water ice cap enlarged by 5° latitude or by using present-day orbit (and thus a warmer southern summer) result in stronger deposition and ice deposits further east.
- F. Costard, F. Forget, N. Mangold, J. P. Peulvast, *Science* **295**, 110 (2002); published online 29 November 2001 (10.1126/science.1066698).
- D. H. Scott, K. L. Tanaka, *U. S. Geol. Surv. Misc. Invest. Map I-1802-A* (1986).
- The LMD Martian global climate model has been developed with the support of CNRS, European Space Agency (ESA), and CNES in collaboration with the Atmospheric, Oceanic, and Planetary Physics group in Oxford University (UK). Much of this work was performed while F.F. was visiting the Space Science Division of NASA Ames Research Center as a Senior National Research Council fellow. We wish to thank J. Hollingsworth, J. Schaeffer, T. Colaprete, and C. P. McKay for their support and advice. The research was also strongly motivated by the recent results from the ESA Mars Express mission within the scope of the Interdisciplinary Scientist Program. J.W.H. thanks the NASA Mars Data Analysis Program for partial support.

Supporting Online Material

www.sciencemag.org/cgi/content/full/311/5759/368/DC1
Figs. S1 to S3

19 September 2005; accepted 15 December 2005
10.1126/science.1120335

South-Seeking Magnetotactic Bacteria in the Northern Hemisphere

Sheri L. Simmons,^{1,2} Dennis A. Bazylinski,³ Katrina J. Edwards^{2*}

Magnetotactic bacteria contain membrane-bound intracellular iron crystals (magnetosomes) and respond to magnetic fields. Polar magnetotactic bacteria in vertical chemical gradients are thought to respond to high oxygen levels by swimming downward into areas with low or no oxygen (toward geomagnetic north in the Northern Hemisphere and geomagnetic south in the Southern Hemisphere). We identified populations of polar magnetotactic bacteria in the Northern Hemisphere that respond to high oxygen levels by swimming toward geomagnetic south, the opposite of all previously reported magnetotactic behavior. The percentage of magnetotactic bacteria with south polarity in the environment is positively correlated with higher redox potential. The coexistence of magnetotactic bacteria with opposing polarities in the same redox environment conflicts with current models of the adaptive value of magnetotaxis.

Magnetotactic bacteria form intracellular single-domain ferrimagnetic iron oxide (magnetite, Fe₃O₄) or iron sulfide (greigite, Fe₃S₄) crystals. The torque produced by these chains causes the cells to align and to

swim with respect to local or induced magnetic fields (1-3). Magnetotactic bacteria are globally distributed at and below the oxic-anoxic interface in chemically stratified freshwater (4-6) and marine environments (7-10), where they can

reach significant population densities (10^5 cells ml^{-1}) (4, 11). Magnetotaxis is currently thought to enable these bacteria to more rapidly locate habitats with low or no oxygen in a vertical chemical and/or redox gradient (12). Here we describe observations that call into question this explanation for the adaptive value of magnetotaxis.

There are two predominant types of magnetotaxis in magnetotactic bacteria: **polar and axial** (12). When observed microscopically in an applied magnetic field, a polar magnetotactic bacterium swims in a preferred direction relative to the local field, whereas an axial bacterium swims back and forth in both directions (12). When the direction of an applied field is reversed, a polar bacterium reverses swimming direction, whereas an axial bacterium rotates 180° but continues to swim back and forth (12). Axial behavior has only been observed in cultivated strains of the genus *Magnetospirillum* (12–14), whereas polar behavior is exhibited far more commonly by magnetotactic bacteria in marine samples (15). The polarity of polar magnetotactic bacteria is defined as their swimming direction under atmospheric oxygen levels. Here we explore the environmental cues that influence polarity among magnetotactic bacteria.

Previous work asserted that virtually all polar magnetotactic bacteria (>99%) in the **Northern Hemisphere** have north polarity (1, 16, 17), which means that they **swim toward geomagnetic north when exposed to higher than optimal oxygen levels**. In the Northern Hemisphere, owing to the vertical component of the Earth's geomagnetic field, swimming toward geomagnetic north would direct bacteria downward into anoxic sediments or waters in a vertical chemical gradient. In the **Southern Hemisphere**, **polar magnetotactic bacteria swim toward geomagnetic south**, presumably for the same reason (2, 3). Here we report observing significant numbers of magnetotactic bacteria in the Northern Hemisphere that swim toward geomagnetic south when exposed to high oxygen (south polarity), the opposite of all previously described magnetotactic behavior. We also show that south polarity in magnetotactic bacteria is statistically correlated with environmental redox chemistry.

A morphologically unusual bacterium with south polarity was found at high density in Salt Pond (Falmouth, MA), a small, seasonally stratified marine basin, in July 2004 (18). This bacterium ("barbell") formed chains of two to five cocci, which appeared refractive with differential

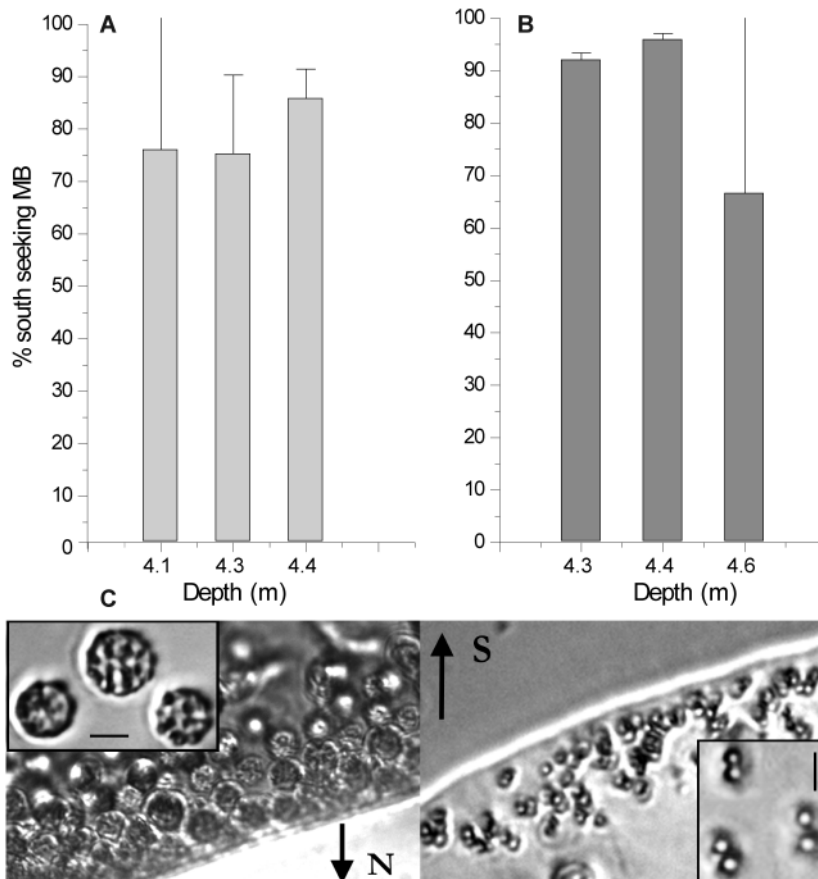


Fig. 1. The barbell and small rod-shaped cells (not shown) have primarily south polarity at discrete depths in Salt Pond. % S seekers is $100 \times$ the ratio of magnetotactic bacteria with south polarity to total magnetotactic bacteria. The mean and standard deviation were calculated from microscopic counts of two drops from the same sample. In both samples, higher standard deviation was associated with low total cell counts. (A) A small rod-shaped magnetotactic bacterium had south polarity in Salt Pond on 1 July 2004. (B) Barbells had south polarity in Salt Pond on 2 July 2004. (C) MMP with north polarity (left) and barbells with south polarity (right) co-occurring in water from Salt Pond on 2 July 2004. Insets show cell morphology. All scale bars, $5 \mu\text{m}$.

interference contrast (DIC) microscopy (Fig. 1C). The barbell occurred in narrow layers immediately below the oxygen-sulfide interface in Salt Pond and cooccurred with previously described magnetite- and greigite-producing bacteria (9) (Fig. 1C). Magnetotactic bacteria were not present at depths above and below those shown in Fig. 1.

Because of the high cell density ($4.6 \pm 1.1 \times 10^4$ cells ml^{-1} , on the basis of direct counts), we were able to observe the polarity of the barbell without potential interference from prior magnetic enrichment (18). Over 90% of the barbells from bulk water samples showed south polarity in the standard drop assay (18) (Fig. 1B). Morphologically distinct populations with north polarity cooccurred with the barbell, which suggests that south polarity was not universal among all magnetotactic bacterial taxa in a given environment (Fig. 1C).

We identified the barbell as a member of the *Desulfobulbaceae* family of the delta *Proteobacteria* (Fig. 2), using sequencing of 16S ribosomal DNA (rDNA) and catalyzed reporter deposition–

in situ hybridization (CARD-FISH) with custom-designed probes (18). It is closely related to *Desulforhopalus singaporensis*, which also has an unusual chain morphology (19). The barbell is the third magnetotactic bacterium identified in the delta *Proteobacteria*; of the other two, one produces magnetite (20) and the other greigite (21).

We also observed a population of small magnetotactic rods with south polarity in Salt Pond on 1 July 2004 (Fig. 1A). These appeared at high density ($1.5 \pm 0.47 \times 10^4$ cells ml^{-1}) at and below the narrow chemocline and had nearly 100% south polarity at every depth at which they occurred. South polarity is not an artifact of our assay; we did not directly observe polarity reversal caused by the small magnets we used, and past experiments have required far higher field strengths (2, 22).

We only observed these dense populations of magnetotactic bacteria with overwhelmingly south polarity on one occasion. Further observations indicated that magnetotactic bacteria more frequently occurred at lower abundance

¹Massachusetts Institute of Technology–Woods Hole Oceanographic Institution (MIT-WHOI) Joint Program in Oceanography, ²Geomicrobiology Group, Department of Marine Chemistry and Geochemistry, MS 52, WHOI, Woods Hole, MA 02543, USA. ³Department of Biochemistry, Biophysics, and Molecular Biology, Iowa State University, Ames, IA 50011, USA.

*To whom correspondence should be addressed. E-mail: katrina@whoi.edu

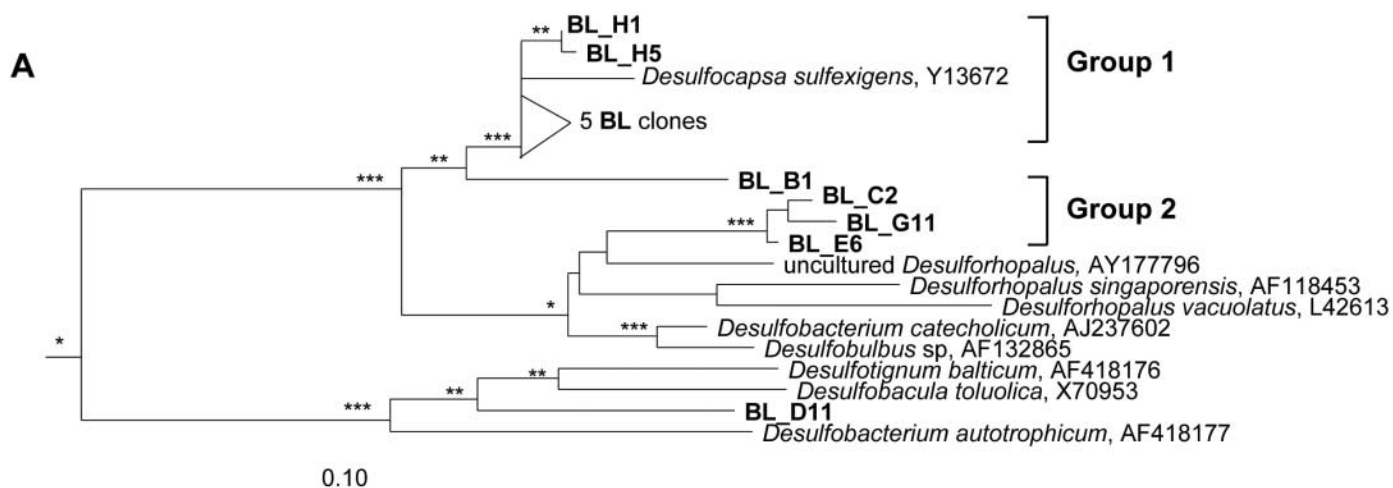
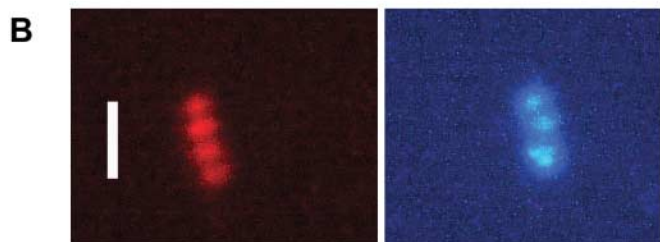
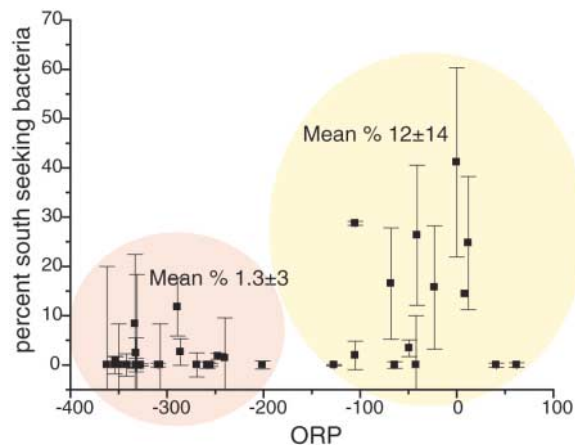


Fig. 2. The barbell was identified as a delta proteobacterium by using CARD-FISH. (A) Two clusters of 16S rDNA sequences (marked with BL_*) were obtained from samples highly enriched in the barbell bacterium. GenBank sequence accession numbers are listed in (23). The tree was constructed using maximum likelihood analysis and 1000 bootstrap replicates in Phylip. Nodes with greater than 90% bootstrap support are marked with ***, 60 to 90% with **, and 50 to 60% with *. A mask was used to allow for inclusion of partial sequences (700 to 800 bp), and sequences were exported from ARB with a 25% homology filter based on a complete alignment of delta Proteobacteria. *Desulfovibrio desulfuricans* was used as an outgroup to root the tree (not shown). Short sequences were added using the ARB Parsimony tool without changing tree topology. Parsimony analysis also supported the tree topology. (B) Left, the barbell with south polarity hybridizes with a



horseradish peroxidase (HRP)-labeled probe (visualized with Cy3-tyramides) targeting group 2 sequences (related to *Desulforhopalus* spp.). Right, a DAPI stain of the same cell. Scale bar, 5 μ m.

Fig. 3. South polarity is related to environmental ORP. The percentage of bacteria with south polarity is shown versus the oxidation-reduction potential of Salt Pond in situ water for all magnetotactic bacteria present in the water column for each of five dates in August and September 2005. Percentages were calculated as the total number of bacteria with south polarity divided by the total number of bacteria in three separate drops. The mean is shown \pm one standard deviation. Experimental error (the variation from three separate drops) and statistical error ($1/\text{total number of cells counted}$) were calculated for all points, and the larger value is shown. The yellow oval denotes data points with ORP $>$ -200 , and the pink oval denotes data points with ORP $<$ -200 . As a general trend, most of the counts at ORP $>$ -200 are for magnetotactic cocci and barbells. In 2005, the barbell did not occur at high levels comparable to our observation in 2004.



and showed a mixture of north and south polarities, with occasional blooms dominated by specific taxa. Quantitative polymerase chain reaction (PCR) on samples taken from Salt Pond in summer 2003 (11) showed that abundances of the barbell fluctuate greatly during the seasonal stratification of Salt Pond. The barbell is most abundant when the pond is less stratified, in the early and late season

(10^4 to 10^5 cells ml^{-1}). This is consistent with our observations of dense populations of the barbell and an unidentified small rod early in summer 2004, when the chemocline was very narrow. The sharp chemocline may have contributed to the high abundance of bacteria with south polarity.

To determine whether water chemistry is correlated with the presence of magnetotactic

bacteria with south polarity, we determined the total numbers of magnetotactic bacteria with north and south polarity across the Salt Pond chemocline in summer 2005 in conjunction with fine-scale physical and chemical profiling (18). The oxidation-reduction potential (ORP), collected in situ, provided a bulk descriptor of water chemistry; more negative values indicate a more reducing environment. Total numbers of magnetotactic bacteria peaked between ORP values of -50 and -200 .

We found a significant relationship between ORP and the percentage of magnetotactic bacteria with south polarity (Fig. 3). In more reducing conditions (ORP $<$ -200), the average percentage of bacteria with south polarity was 1.3 ± 3 . Greigite-producing organisms predominated in this group. In more oxidizing conditions (ORP $>$ -200), the average percentage of bacteria with south polarity was 12 ± 14 . The barbell and small magnetite-producing cocci predominated in this group, and most organisms with south polarity were barbells. The high variance is due to the dominance of cocci with north polarity in some samples. The means of the two groups were significantly different at the $P = 0.01$ level (independent t test). There was no correlation between polarity and the total numbers of magnetotactic bacteria observed. Our results suggest that either the polarity of a single bacterium is affected by ORP (or a redox active chemical species correlated

with ORP), or that south polarity is characteristic of a particular species that occurs at a specific ORP.

The coexistence of magnetotactic bacteria with north and south polarity in the same chemical environment contradicts the current accepted model of magnetotaxis, which states that all magnetotactic bacteria in the Northern Hemisphere swim north (downward in situ) when exposed to oxidized conditions to reach their preferred microaerobic or anaerobic habitat. We observed that barbells with south polarity and cocci with north polarity coexist in microaerobic conditions in the water column. On the basis of this distributional pattern, south polarity is clearly not used to direct the barbell upward in the water column toward higher oxygen levels. The current model does not, therefore, provide any explanation that can account for the existence of south polarity.

This model implicitly assumes that polarity observed in the laboratory under atmospheric oxygen levels is equivalent to polarity in situ. Our results suggest that this assumption might be incorrect. Although the benefit of north polarity in situ is clear for microaerophilic magnetotactic bacteria, south polarity would have a clearly deleterious effect by directing the bacteria away from their preferred chemical environment. There are reasons to believe the behavior of magnetotactic bacteria in situ could differ from behavior in the laboratory. Magnetotactic bacteria at the chemocline of a stratified water column

rarely, if ever, experience atmospheric oxygen levels like those in the standard laboratory assay for polarity. They also experience chemical gradients (particularly of iron and sulfur species) not present in a drop of water exposed to air in the laboratory assay. It is also possible that bacteria with north and south polarity possess different chemo- or redox-sensors that have opposite responses to chemical concentrations out of the range they typically experience. On the basis of these results, new models are clearly needed to explain the adaptive significance of magnetotaxis by magnetotactic bacteria in the environment.

References and Notes

1. R. P. Blakemore, *Annu. Rev. Microbiol.* **36**, 217 (1982).
2. R. P. Blakemore, R. B. Frankel, A. J. Kalmijn, *Nature* **286**, 384 (1980).
3. J. L. Kirschvink, *J. Exp. Biol.* **86**, 345 (1980).
4. S. Spring *et al.*, *Appl. Environ. Microbiol.* **59**, 2397 (1993).
5. S. Spring, R. Amann, W. Ludwig, K.-H. Schleifer, N. Petersen, *Syst. Appl. Microbiol.* **15**, 116 (1992).
6. T. Sakaguchi, A. Arakaki, T. Matsunaga, *Int. J. Syst. Evol. Microbiol.* **52**, 215 (2002).
7. H. Petermann, U. Bleil, *Earth Planet. Sci. Lett.* **117**, 223 (1993).
8. J. F. Stolz, S.-B. R. Chang, J. L. Kirschvink, *Nature* **321**, 849 (1986).
9. S. L. Simmons, S. M. Sievert, R. B. Frankel, D. A. Bazylinski, K. J. Edwards, *Appl. Environ. Microbiol.* **70**, 6230 (2004).
10. D. A. Bazylinski *et al.*, *Appl. Environ. Microbiol.* **61**, 3232 (1995).
11. S. L. Simmons, K. J. Edwards, manuscript in preparation.
12. R. B. Frankel, D. A. Bazylinski, M. S. Johnson, B. L. Taylor, *Biophys. J.* **73**, 994 (1997).

13. R. P. Blakemore, D. Maratea, R. S. Wolfe, *J. Bacteriol.* **140**, 720 (1979).
14. A. M. Spormann, R. S. Wolfe, *FEMS Microbiol. Lett.* **22**, 171 (1984).
15. S. L. Simmons, K. J. Edwards, unpublished observations.
16. R. P. Blakemore, *Science* **190**, 377 (1975).
17. T. T. Moench, W. A. Konetka, *Arch. Microbiol.* **119**, 203 (1978).
18. Materials and methods are available as supporting material on Science Online.
19. T. J. Lie, M. L. Clawson, W. Godchaux, E. R. Leadbetter, *Appl. Environ. Microbiol.* **65**, 3328 (1999).
20. R. Kawaguchi *et al.*, *FEMS Microbiol. Lett.* **126**, 277 (1995).
21. E. F. DeLong, R. B. Frankel, D. A. Bazylinski, *Science* **259**, 803 (1993).
22. A. J. Kalmijn, R. P. Blakemore, in *Animal Migration, Navigation, and Homing*, K. Schmidt-Koenig, W. Keeton, Eds. (Springer-Verlag, Berlin, 1978), pp. 354-355.
23. We thank P. Canovas and O. Rafie for field and lab assistance; R. Frankel, E. Webb, and S. Sievert for input on the manuscript; and K. Canter for use of a magnetometer. S.L.S. was partially supported by a National Defense Science and Engineering Graduate Fellowship. This work was partially funded by grants to S.L.S. and K.J.E. from the WHOI Reinhart Coastal Research Center, the WHOI Ocean Venture Fund, and the WHOI Ocean Life Institute. D.A.B. is supported by National Science Foundation grant EAR-0311950. GenBank sequence accession numbers for the sequences reported in this study are as follows. Group 1: BL_G6, DQ322653; BL_H12, DQ322654; BL_H1, DQ322655; BL_H4, DQ322662; BL_H5, DQ322656; BL_C10, DQ322657; BL_C5, DQ322658. Group 2, south-seeking bacterium: BL_C2c, DQ322659; BL_E6c, DQ322660; BL_G11c, DQ322661.

Supporting Online Material

www.sciencemag.org/cgi/content/full/311/5759/371/DC1

Materials and Methods
References

21 November 2005; accepted 20 December 2005
10.1126/science.1122843

Sampling the Antibiotic Resistome

Vanessa M. D'Costa,¹ Katherine M. McGrann,¹ Donald W. Hughes,² Gerard D. Wright^{1*}

Microbial resistance to antibiotics currently spans all known classes of natural and synthetic compounds. It has not only hindered our treatment of infections but also dramatically reshaped drug discovery, yet its origins have not been systematically studied. Soil-dwelling bacteria produce and encounter a myriad of antibiotics, evolving corresponding sensing and evading strategies. They are a reservoir of resistance determinants that can be mobilized into the microbial community. Study of this reservoir could provide an early warning system for future clinically relevant antibiotic resistance mechanisms.

Most clinically relevant antibiotics originate from soil-dwelling actinomycetes (*I*). Antibiotic producers harbor resistance elements for self-protection that are often clustered in antibiotic biosynthetic operons (2, 3). Genes orthologous to these have been identified on mobile genetic elements in resistant pathogens in clinical settings. It has been sug-

gested that aminoglycoside-modifying kinases (4) and the alternate peptidoglycan biosynthetic machinery that confers resistance to vancomycin (5) probably originated in soil-dwelling antibiotic producers.

The presence of antibiotics in the environment has promoted the acquisition or independent evolution of highly specific resistance elements in the absence of innate antibiotic production [such as vancomycin resistance in *Streptomyces coelicolor*, *Paenibacillus*, and *Rhodococcus* (6, 7)]. The soil could thus serve as an underrecognized reservoir for resistance that has already emerged or has the potential

to emerge in clinically important bacteria. Consequently, an understanding of resistance determinants present in the soil—the soil resistome—will provide information not only about antibiotic resistance frequencies but also about new mechanisms that may emerge as clinical problems.

We isolated a morphologically diverse collection of spore-forming bacteria from soil samples originating from diverse locations (urban, agricultural, and forest). Strains that resembled actinomycetes both morphologically and microscopically were serially subcultured to apparent homogeneity. Amplification and sequencing of 16S ribosomal DNA from a subset of strains indicated that they belonged to the actinomycete genus *Streptomyces*, whose species synthesize over half of all known antibiotics (*I*). We constructed a library of 480 strains that was subsequently screened against 21 antibiotics, including natural products (such as vancomycin and erythromycin), their semisynthetic derivatives (such as minocycline and cephalixin), and completely synthetic molecules (such as ciprofloxacin and linezolid). The antibiotics encompassed all major bacterial targets (8) and included drugs

¹Antimicrobial Research Centre, Department of Biochemistry and Biomedical Sciences, ²Department of Chemistry, McMaster University, Ontario, Canada, L8N 3Z5.

*To whom correspondence should be addressed. E-mail: wrightge@mcmaster.ca